A Three-Dimensional Parametric Adult Head Model with Representation of Scalp Shape Variability Under Hair

Byoung-Keon D. Park, Brian D. Corner, Jeffrey A. Hudson, Jennifer Whitestone, Casserly R Mullenger, Matthew P. Reed

GRAPHICAL ABSTRACT

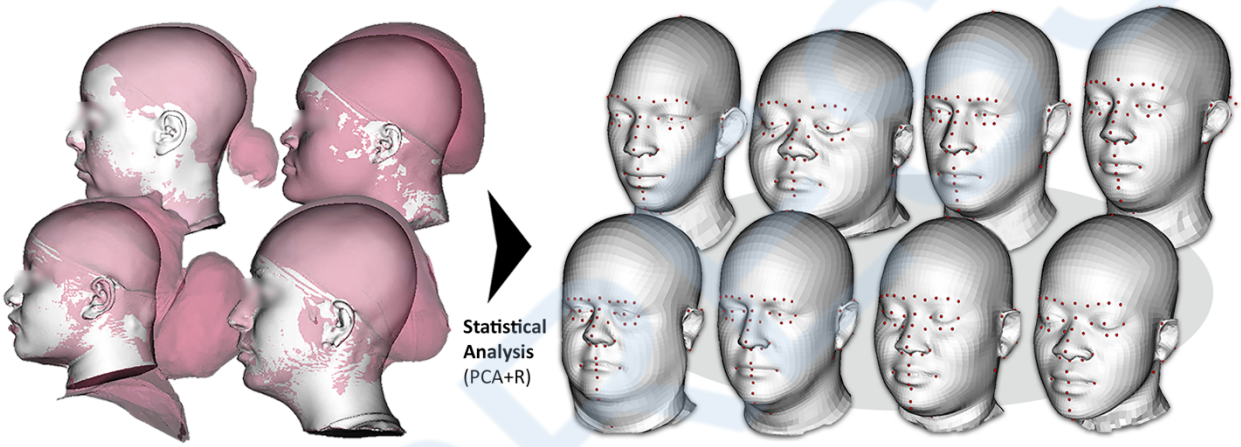

Source data: Head scans under hair

Random head shapes generated using developed model

ABSTRACT

Modeling the shape of the scalp and face is essential for the design of protective helmets and other head-borne equipment. However, head anthropometry studies using optical scanning rarely capture scalp shape because of hair interference. Data on scalp shape is available from bald men, but female data are generally not available. To address this issue, scalp shape was digitized in an ethnically diverse sample of 100 adult women, age 18-59, under a protocol that included whole head surface scanning and scalp measurement using a three-dimensional (3D) coordinate digitizer. A combined male and female sample was created by adding 3D surface scans of a similarly diverse sample of 80 bald men. A statistical head shape model was created by standardizing the head scan data. A total of 58 anatomical head landmarks and 12 head dimensions were obtained from each scan and processed along with the scans. A parametric model accounting for the variability of the head shape under the hair as a function of selected head dimensions was developed. The full-variable model has a mean shape error of 3.8 mm; the 95th percentile error was 7.4 mm, which were measured at the vertices. The model will be particularly useful for generating a series of representing a target population as well as for generating subject-specific head shapes along with predicted landmarks and dimensions. The model is publicly available online at http://humanshape.org/head/.

INTRODUCTION

Three-dimensional (3D) surface scanning technology enables rapid capture of the 3D morphology of an individual's head. Digital head shape models based on head geometry and anthropometry have been used to develop and test products such as helmets (Corner et al. 1997, Liu et al. 2008, Willinger et al. 2002, Friess and Bradtmiller, 2003), Eyeware (Kouchi et al. 2004), mask (Gotoa et al. 2015), and headsets (Lacko et al. 2017). Statistical analysis methods have been employed in these studies to characterize head shape variation and to identify similarities and differences within a large sample 3D anthropometric data. For example, principal component analysis (PCA) provides an efficient way to represent a large dataset of high-resolution head and face scan data with an optimized model (Lacko et al. 2017, Gotoa et al. 2015, Zhuang et al. 2013, Friess and Bradtmiller, 2003). PCA models have typically been used for the quantitative identification of the head shape variance for a target population to facilitate product design.

One major limitation of 3D contactless scanning techniques for obtaining head shape, such as laser scanning, is they rarely capture the scalp surface because the imaging system does not penetrate through hair. Most head shape studies use an elastic cap that compresses hair, but this does not entirely remove the effects of hair on the head surface shape. Some studies have used CT or MRI image databases to resolve this issue (Lacko et al. 2015; Yang et al. 2014; Li et al. 2015; Danckaers et al. 2017). However, only a small number of CT/MRI databases are publicly available from narrow populations (Shah and Luximon 2018). Most importantly, medical imaging rarely captures the entire head and face in the same scan due to concerns about scanning speed and radiation exposure.

This paper presents a parametric head shape model based on a statistical analysis of a large sample of adult head scans that are not contaminated with hair artifacts. These high-resolution head scans of a total of 180 female and male adults were standardized using a template-based fitting method. A PCA and a multivariate regression analysis were conducted using the head geometry along with 58 anatomical landmarks, 12 anthropometric dimensions, and subject demographic data. The main contributions of the work are:

- A statistical head shape model based on a large male bald head scan dataset and a large dataset of female 3D head scans with scalp surface data obtained using a FARO arm,
- regression models representing scalp and face shape given anthropometric dimensions were built using different variable sets, and
- We present a spatial error metric in head shape prediction produced from both PCA and regression models that accounts for the geometric discrepancy between predictions and actual shapes.

METHODS

Data Source

A total of 180 adult bald 3D head scans (100 female and 80 male) subjects with the ethnic diversity of 18 and 59 years old were used for the current analysis. Each scan has about 50K - 100K vertices to describe the 3D scalp shape as well as the face, ears, and neck. Male scalp shapes were obtained from laser-scan studies that included bald men (Gordon et al. 2013, Gordon et al. 2014, unpublished US Army data). The female scalp shapes were obtained under the Air Force IRB approved protocol FWR20060075H using a novel manual digitization method shown in Figure 1 (Mullenger & Hudson 2015). The Artec Eva Scanner (http://artec3d.com) was used to collect initial head scans of subjects, and a FARO Arm coordinate digitizer (Faro Technologies Inc. http://www.faro.com/) was used to record streams of 3D data points on the scalp while the subject's head rested in a stabilizing fixture to limit head movement (Figure 1 (a)). The scalp points were probed through four to five hair parts on each side of the midsagittal plane for a total of ~200 data points. The scalp point data were interpolated as a surface using the thin plate spline technique. The scalp surface was aligned with the 3D scan of the head and face based on the four digitized landmark points (right and left Tragion, Pronasale, and Sellion) and combined to obtain a full head surface. Standard anthropometric values commonly available from both the male and female data sources are head circumference, head length, head breadth, and tragion to top-of-head. Table 1 shows the summary statistics of the data source, and Table 2 shows the subject's ethnicity distribution.

Fifty-eight anatomical head landmarks (Figure 2 and Appendix A) were manually digitized from each scan using MeshLab software (http://meshlab.net). These landmarks are essential for the alignment of the scans to have the same coordinate system and for standardization of the mesh structure to ensure anatomical homology across the scan data, which is critical for statistical analysis. Each landmark was carefully digitized based on rigorous definitions referencing relevant literature (Appendix A), and multiple measurers cross-checked landmark consistency across the scans.

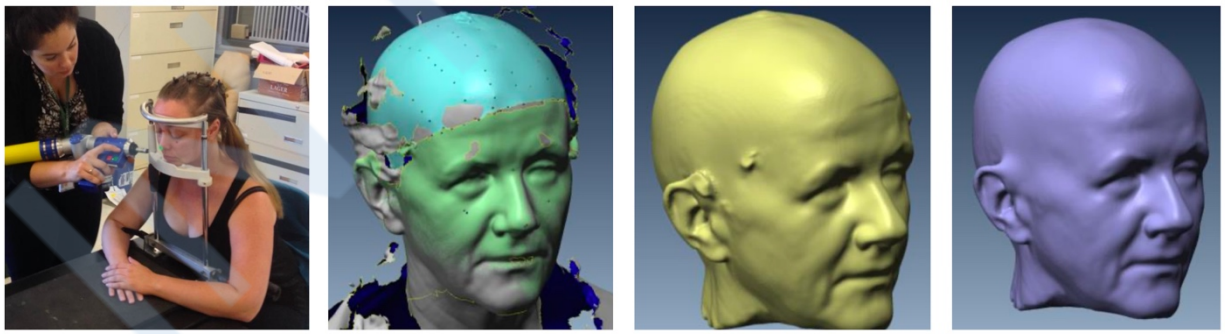

Figure 1. The overall process of female head data acquisition: (a) Obtain a head scan with a portable surface scanner, record four face and calvarium pre-marked anatomical landmarks using a 3D coordinate digitizer as alignment references, then capture scalp surface along five hair parts and along the hairline, (b) generate a scalp surface using a thin plate spline surface warping technique and the eight landmarks to align surface scan and coordinate data, (c) clean and merge scans, and (d) smooth local surface to remove artifacts (Mullenger & Hudson 2015).

Table 1. Head anthropometry descriptive statistics (n=180)

		Mean	SD	Min	Max	5th	95th
Male	Head Breadth (mm)	155.1	5.4	143.0	175.0	145.5	165.0
	Head Circ. (mm)	575.0	15.2	545.0	615.0	553.0	604.5
	Head Length (mm)	200.5	6.6	187.0	224.0	190.5	212.5
	Breadth-to-Length	0.77	0.03	0.71	0.84	0.72	0.84
	Age (YO)	35.6	9.3	19.0	56.0	22.0	52.5
Female	Head Breadth (mm)	146.6	5.8	134.0	165.0	137.0	156.8
	Head Circ. (mm)	556.8	19.3	509.0	610.0	522.6	590.0
	Head Length (mm)	186.5	8.8	152.0	202.0	172.0	200.0
	Breadth-to-Length	0.79	0.04	0.70	0.96	0.72	0.86
	Age (YO)	27.7	10.2	18.0	59.0	19.0	50.8

Table 2. Ethnicity/race of the subjects

Ethnicity/Race	Male	Female	Total
Asian/Pacific Islander	2	14	16 (8.9%)
Black/African American	32	13	45 (25%)
White/Caucasian	33	65	98 (54.4%)
Hispanic	3	4	7 (3.9%)
Others	10	4	14 (7.8%)

All the scans were aligned to a coordinate system that originated at the mid-tragion (Figure 2). The coordinate system was defined at the Frankfurt plane, which is a horizontal plane passing through left and right tragion and right infraorbitale landmarks, given by:

- **Origin**: Midtragion (Mid-point between right and left tragions)
- **Y**(Medial-Lateral): Right tragion to left tragion
- **Z**(Caudal-cephalad): Vertical; obtained as the cross product of the Y axis and the vector from left tragion to left infraorbitale
- **X**(Anterior-Posterior): cross product of the Y and Z axes.

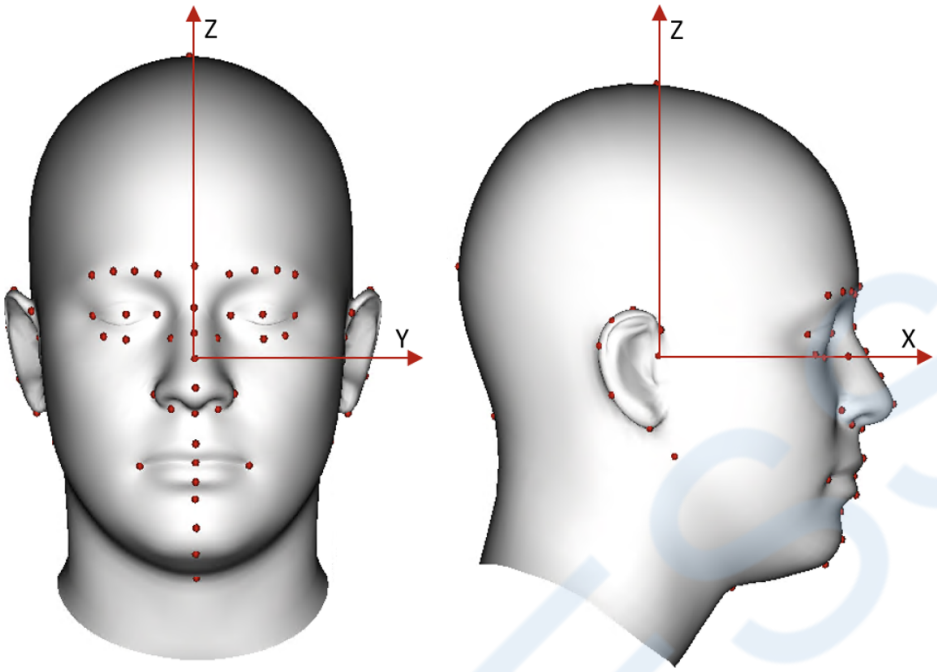

Figure 2. 58 head and face landmarks (red points) on the mean head shape and the global coordinate system originating at the mid-tragion point

There were four traditional anthropometric dimensions, including head length, breadth, circumference, and Tragion to top-of-head, commonly available from both the female and male datasets. All these dimensions were manually measured using the same anthropometric protocol presented in the 2012 U.S. Army Anthropometric Survey (ANSUR II) (Gordon et al. 2014). The definitions of these dimensions are listed in Appendix B

Along with the four manually measured traditional anthropometric dimensions, seven additional dimensions were computed from the scans. An automatic dimension computation algorithm based on landmark locations was developed based on ANSUR II and applied to measure the seven dimensions. For example, Head Arc Length was estimated from the intersecting curve between the scan and a plane passing through Glabella, Occiput, and Top of Head points. All the definitions of these digital dimensions are listed in Appendix B. Table 3 lists the demographic information collected from subjects and traditional head anthropometry measured using manual techniques as well as the digital head dimensions estimated from the scans.

Table 3. Subject demographics, manually measured head anthropometry, and digital head dimensions estimated from 3D scans.

Standard Manual Head Anthropometry and Demographic Data	**Head Anthropometry Estimated from Scans**
Head Length	Bitragion Chin Arc
Head Breadth	Bitragion Submandibular Arc
Head Circumference	Bitragion width
Length-Breadth Ratio	Head Arc Length

Tragion to top-of-head	Face Width
Sex	Ear Height
Age	Arc Width
Ethnicity/Race	

Template-based Standardization

Standardizing the polygonal structure (mesh) of the scans is essential prior to a statistical analysis of the morphologic variance across the head scans. We standardized the head meshes by fitting a template mesh to all the scans using a two-level fitting method (Park and Reed 2015, Park et al. 2017). Briefly, this method first morphs a template model based on the landmarks of the target scan using a radial basis function (RBF) technique. The initial morphing step ensures specific template vertices are located at corresponding landmark locations across all target scans. In a second step, an implicit surface fitting technique fits the morphed template to a target scan and captures geometric detail. The template head shape model has a symmetric mesh structure with 5487 vertices (Figure 3b).

We also applied two additional refinement processes -- imposing right-left symmetry and ear shape reconstruction -- to improve final model usability. The template-fit meshes were made right-left symmetric by averaging right-left paired coordinate vertices. The landmark data were also repositioned to be right-left symmetrical using an RBF technique that accounted for vertex movements. Finally, ear geometry was refined to eliminate scanning artifacts due to the inherent geometrical complexity. We morphed the ear parts extracted from the template model to each scan based on manually digitized ear landmark data.

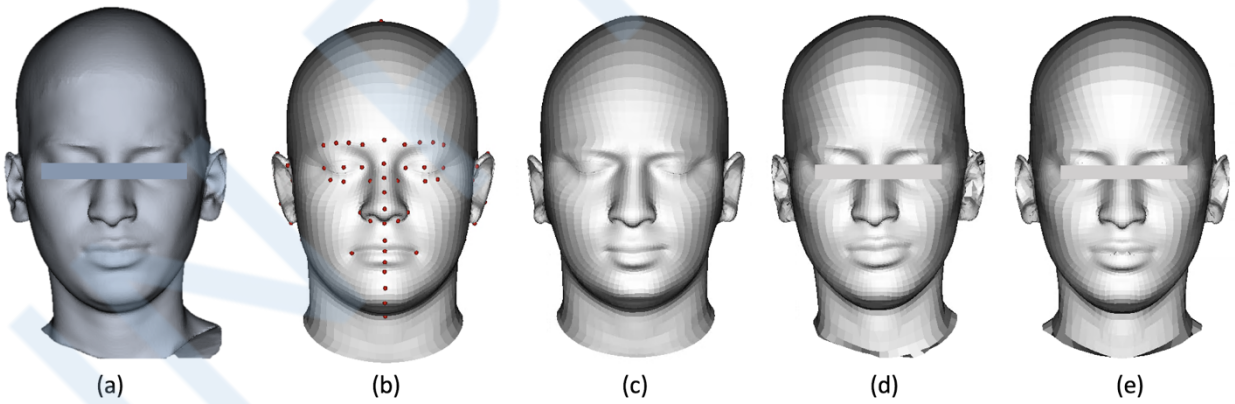

Figure 3. Template fitting process: (a) target scan, (b) template model with landmarks, (c) initial template morph based on landmarks, (d) fine-fitted model, and (e) final symmetric fit

Statistical Head Shape Model

The processed mesh data were statistically analyzed using principal component (PC) and regression analyses (Park and Reed 2015). First, the 12 anthropometric head dimensions, three demographic data, the coordinates of the 58 measured landmarks, and the 5487 model vertices for each fit were merged as a one-dimensional geometric vector. Next, the vectors were run through a PC analysis. The geometric vectors were then projected to the PC space yielding PC

coordinates (scores) for each subject. Finally, a multivariate regression model was built using standard ordinary least squares methods to associate the projected PC scores with anthropometric predictors, e.g., head length, breadth, and circumference. The regression allows the head shape model to be intuitively manipulated with standard head dimensions.

RESULTS

The effect of the number of PCs used for reconstruction was examined to determine a number that yields an acceptable error. Our error metric was defined as the Euclidean distances from the vertices of a head model reconstructed with a given number of the PC scores to the corresponding nodes of the original template-fit head. Figure 4 shows the quantiles of the unsigned errors as the number of PCs varied from 170 to 10. The median mean errors (Figure 4a) were 1.2 mm for all subjects with 50 PCs and 0.5 mm with 100 PCs. The median 95th percentile errors (Figure 4b) are 2.4 mm and 1.2 mm, respectively. Based on this examination of error, the first 100 PCs, yielding a median 95th-percentile error of 1.2 mm, were used to create the parametric head model. Figure 5 shows head shape variations of the first four principal components at plus and minus three standard deviations.

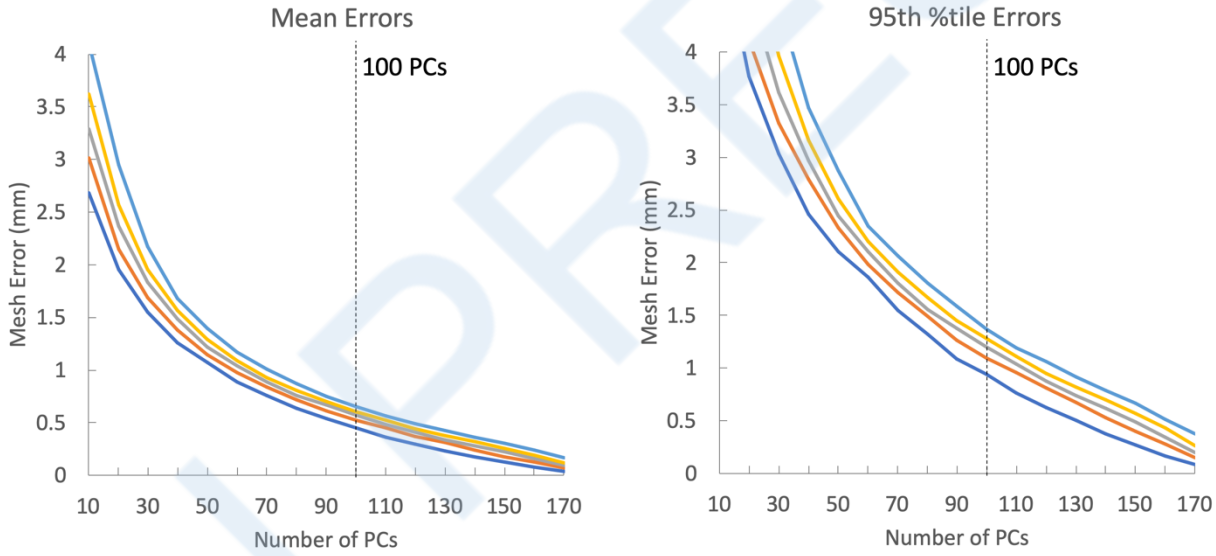

(a) (b)

Figure 4. Effects of the number of retained PCs on quantiles (across subjects) of (a) **mean** error (within-subject) and (b) **95th percentile** errors (within-subject). Quantiles 0.05, 0.25, 0.5, 0.75, and 0.95 are shown.

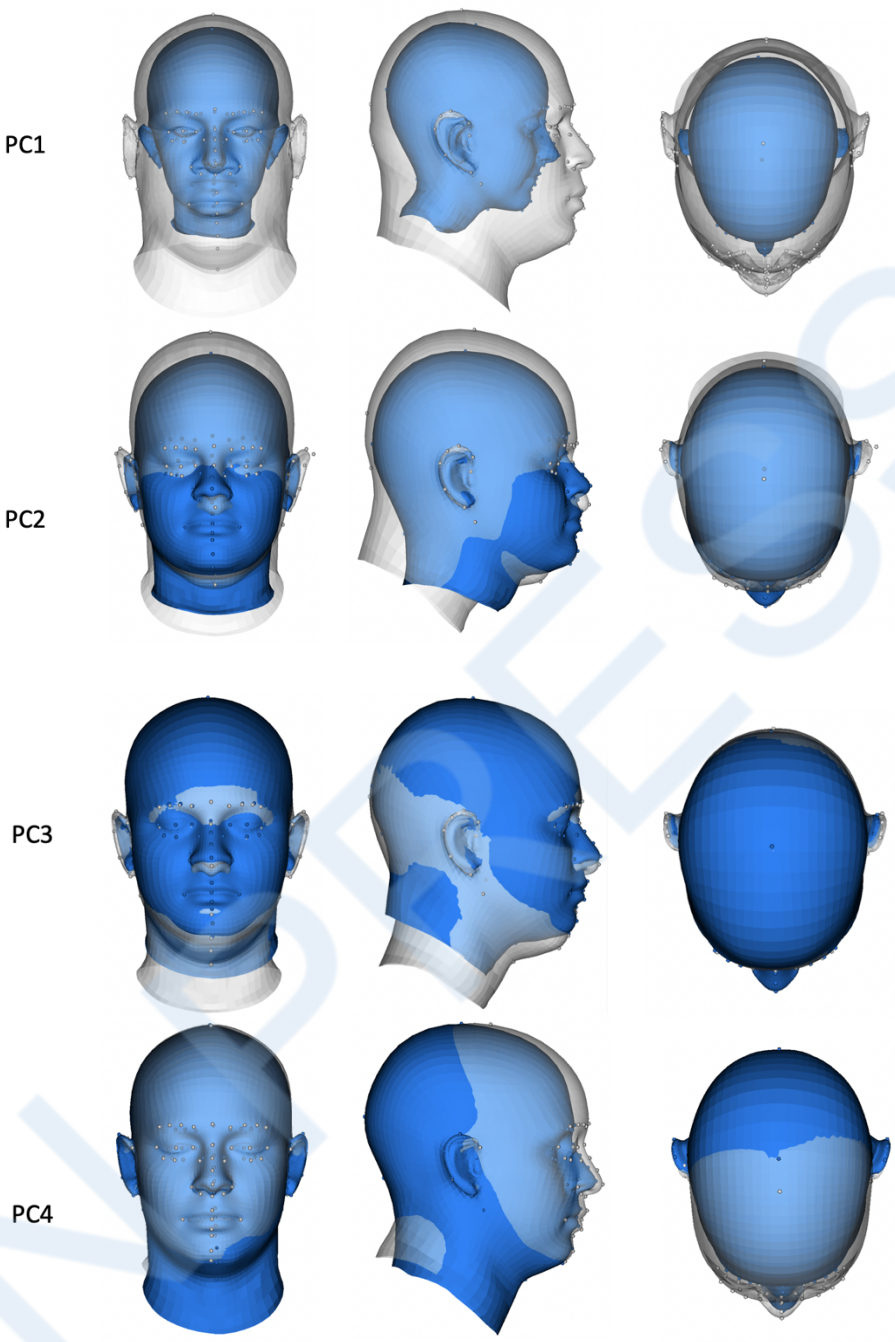

Figure 5. Visualization of the first four principal component effects on the head shape. -3.0σ (blue) and +3.0σ (white) are compared.

Multivariate regression analysis was performed to associate the given 100 PCs with the anthropometric measurements as predictors. Various combinations of anthropometric data could be used as predictors depending on application needs. Figure 6 illustrates the outputs of a

two-variable regression model using *Head Length* and *Chin Arc Length* as predictors for male and female head models.

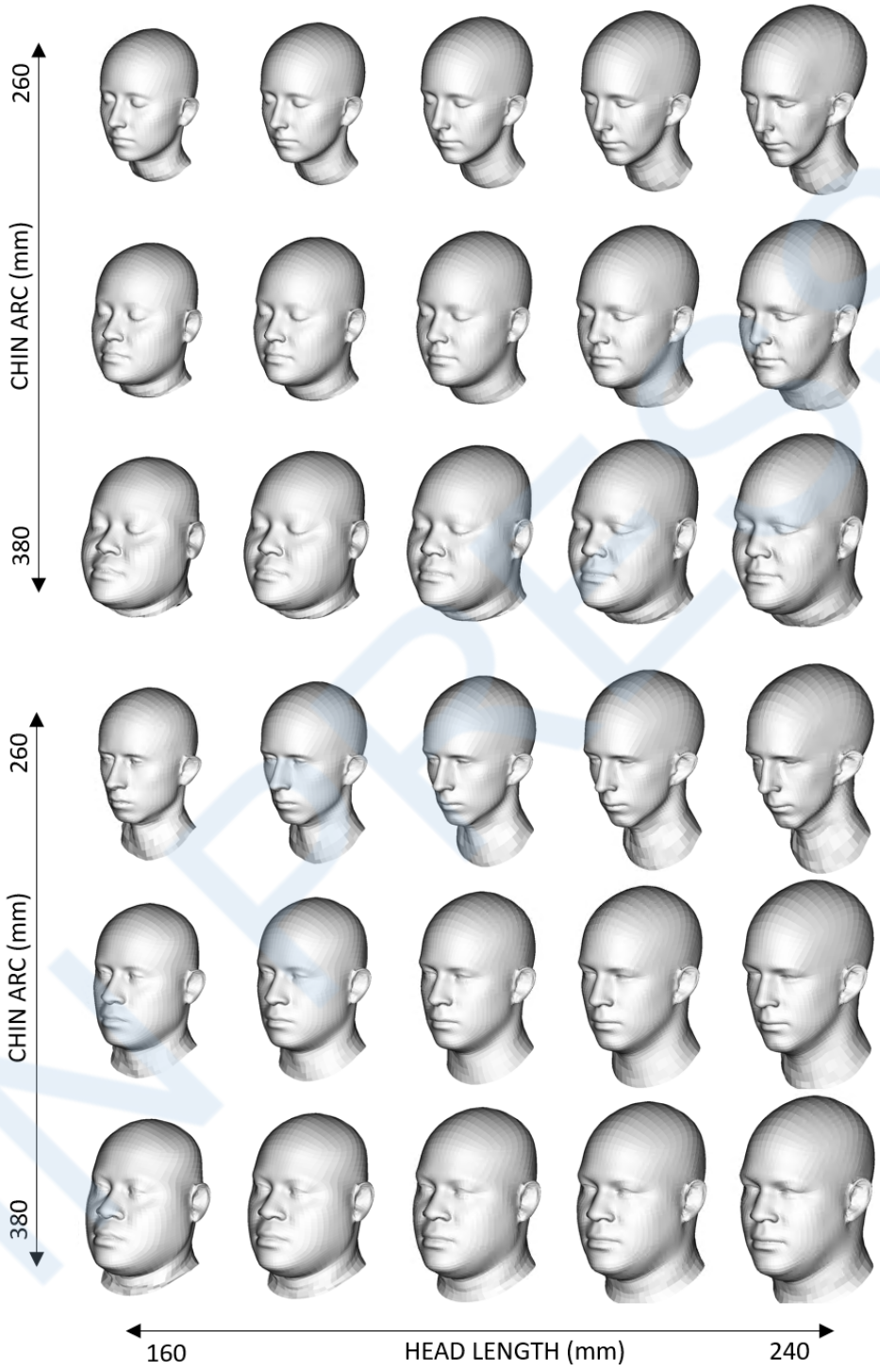

Figure 6. Sample outputs from a two-variable regression head shape model showing a range of head lengths (160 ~ 240 mm) and chin arc lengths (260 ~ 380 mm) on each female (upper) and male (lower) head shape.

Using more variables in the regression can be expected to improve head shape prediction. Figure 7 shows comparisons between a subject scan and predicted shapes using a full-variable regression model and a three-variable model with the parameters of head length, head circumference, and chin arc length. Since the neck posture was not standardized, the neck segment has the most significant prediction error. The scalp and face were predicted with relatively small errors (< 10 mm) even with three variables. Figure 8 shows the cumulative (across subjects) mean and 95th percentile mesh error (within-subject) for the full regression with 14 predictors, with five predictors, and with three predictors. The median mean errors were 3.8 mm, 4.1 mm, and 4.8 mm with 11, 5, 3 predictors, respectively, and the median 95th percentile errors were 7.4 mm, 8.5 mm, 9.0 mm with 11, 5, 3 predictors.

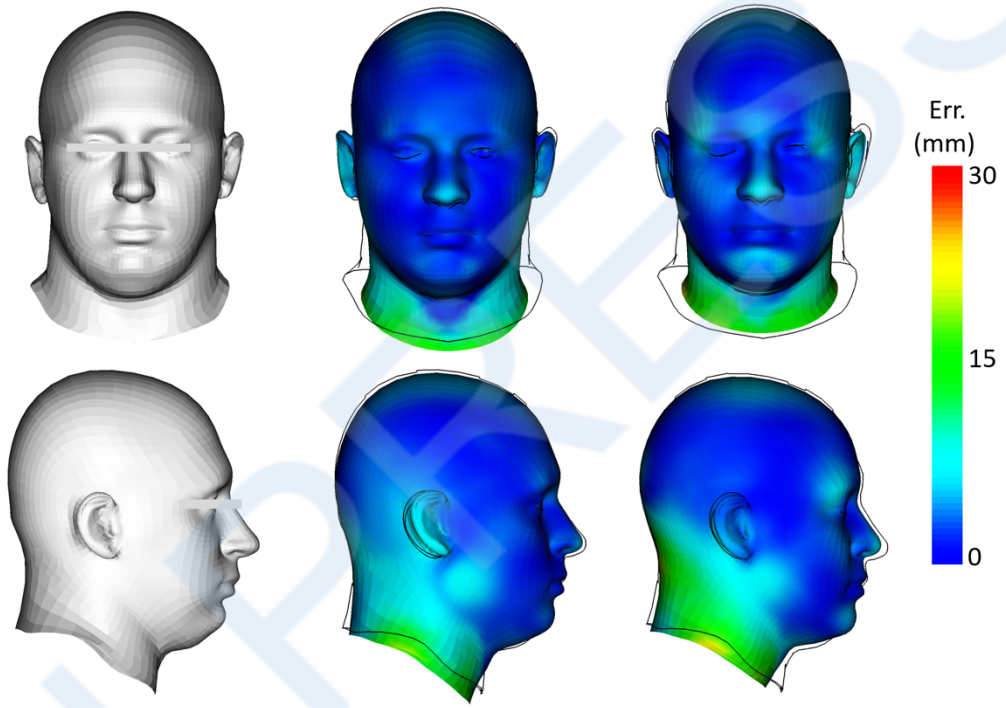

Figure 7. Comparisons between a subject scan (left) and predicted head shapes with a full-variable regression model (middle) and a three-variable regression model (right). Predicted shapes are colorized with a heatmap based on the distance to the scan surface (black lines) at each vertex.

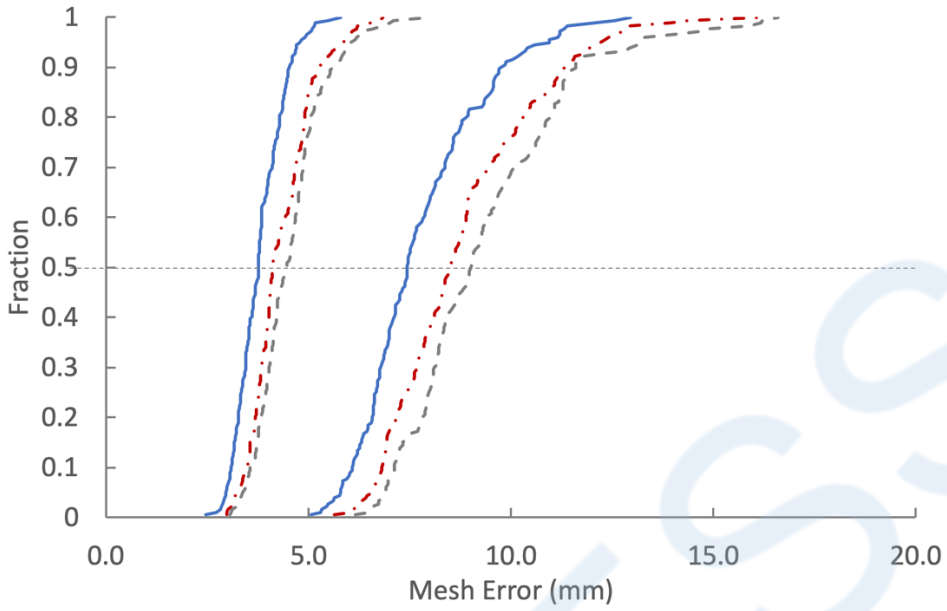

Figure 8. Distribution of mean (left curves) and 95th percentile (right curves) mesh error across subject for regressions with full variables (solid lines), 5 variables (dash-dotted lines), and 3 variables (dashed lines).

This parametric head shape model allows an easy and intuitive generation of a 3D digital head shape along with the 58 landmarks and anthropometric dimensions. For example, ten randomly generated head shape are shown in Figure 9.

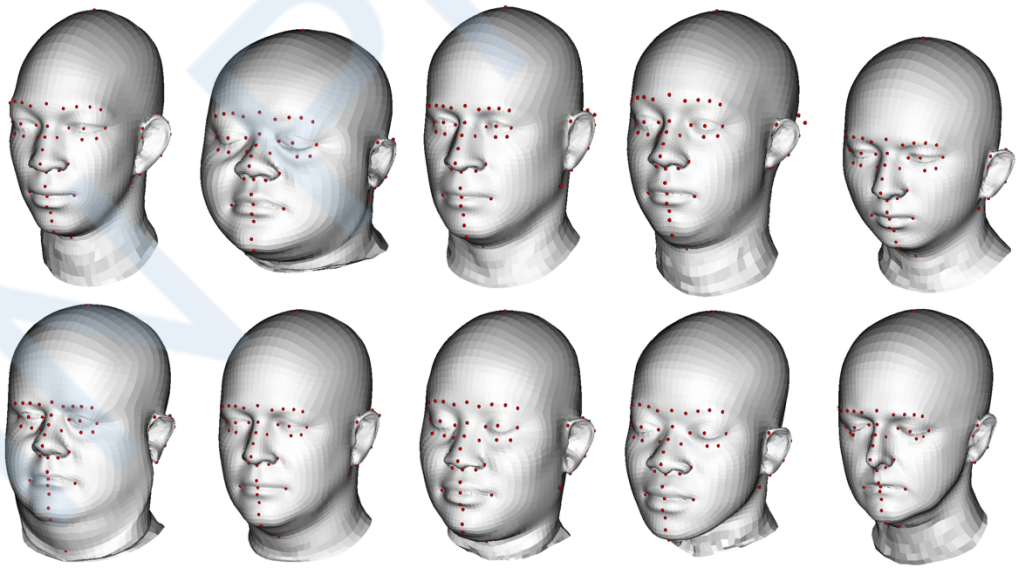

Figure 9. Randomly generated head models with landmarks (red) within the head shape space of the model

DISCUSSION

Our new parametric head shape model accounts for head shape variance without hair artifacts. High-resolution head scans from 180 ethnically diverse female and male adults were used to build the model, which is the largest dataset of bald head scans for a single model to our knowledge. The availability of a large set of well-defined, standardized landmarks is a unique attribute of this model. Consistent landmark data is valuable for obtaining homologous template fits and minimizes prediction accuracy degradation in the final model (Xi and Shu 2009, Marin et al. 2018). More importantly, the availability of the landmarks in the predictions enables a much more extensive range of applications.

An approach to determining the number of PCs for subsequent modeling is to select an arbitrary cutoff in the cumulative variance (Jolliffe, 2002), for example, accounting for 95% of the variance in the underlying data. However, choosing the number of PCs to retain by this method does not provide a practical indication of the effects on the spatial error in shape reconstruction or prediction. To examine this factor, the reconstruction error, quantified as the distance between the reconstructed and original mesh, was calculated across all 180 head scans for a number of PCs ranging from 10 to 170. We selected 100 PCs yielding a median 95th percentile error of 1.2 mm for the model in this study, which means 50% of individuals have a 95th percentile mesh error of less than 1.2 mm. This error criterion was judged to be acceptable for the internal use within the project team while keeping the efficiency of the model, but the number of the PCs and the error criterion can be adjusted based on the needs of a given application. For example, the first 70 PCs yielding a median 95th-percentile error of about 2 mm can be chosen to meet the allowable error for the head length and breadth from the ANSUR II survey. We also note that because the vast majority of the work in the study is measuring the heads, digitizing landmarks, and fitting the data, creating a model for a different application that uses more or fewer PCs (or different predictors) is trivial.

The 100 PCs were then associated with the anthropometric variables as head shape parameters using multivariate regression analysis for an intuitive head shape manipulation. This regression method creates separate equations to predict PC scores. Typical approaches to assess regression model performance, such as significance tests on parameter estimates and analysis of residuals, are not very useful for this application because the dependent measure for each regression is a PC score, rather than an outcome of direct interest. Moreover, testing whether particular variables have “significant” effects on the outcome is not important since the goal is to make predictions.

The residuals of interest are the discrepancies between the predicted and measured head shapes, rather than the residuals from the regressions. We investigated the effects of the number of anthropometric parameters using the same error metric used to evaluate the PC effects. Increasing the number of anthropometric predictors reduces the error only slightly relative to the distribution across subjects, indicating that (1) the selected dimensions capture a large amount of the variance in head size and shape across individuals, and (2) addition dimensions tend to affect relatively small areas of the model. The median 95th percentile error with the full parameters is reduced only from 9 to 7 mm compared with the three-variable regression.

There could be a measurement variability issue by using the manual caliper anthropometric measurements from different sources and different people (inter-observer variability). However,

there also are reasons why we incorporate these manual measurements along with the digital measurements in the model:

- Inter-observer variability was carefully controlled to minimize the human errors in the measurements by collecting the data by a few well-trained measurers for both the male and female datasets. Also, all the measurements were performed following the detailed standardized protocols described in the ANSUR II documentation. We believe the inter-observer variability for these datasets is negligible.
- The caliper measures of head breadth and length are included because these generally differ systematically from measurement that can be made digitally, due to flesh deformation.
- The manual measurement data were used as the input parameters of the model since it is more practical for the majority of users. The head circumference, for example, tends to be measured a bit larger in general than the actual dimension due to the hair effect. However, at the same time, these manually measured dimensions are what the people indeed have for the generation of a subject-specific model. Thus, we decided to incorporate the most commonly manually measured dimensions into the model to make it broadly useful.

The distribution of mesh nodes has an impact on the assessment of anthropometry prediction error for the full head model. For example, the high density of nodes in the eye, nose, and mouth areas compared to the back of the scalp means errors in the face region may dominate the predictions. Also, we observed that a different vertex distribution in the template (baseline) model affects the resulting principal components (PCs) from PCA. In practice, this disparity might affect applications that directly use the PCA model, for example, PC-based shape fitting (Park et al. 2017) or boundary manikin generation in PC space (Reed and Park, 2017). There would be two approaches to resolve the vertex density disparity issue in practice: (1) applying statistical weights differently for the face and scalp vertices, and (2) adjusting point density by subdividing polygons in the scalp area or decimating polygons in the face area. The first approach is easy to implement but requires building another PCA model. The second one does not require building a separate PCA, but attention is needed to choose proper statistical weights. However, we have not found meaningful differences in decision points in this work (for example, choice of the number of PCs to retain) based on reweighting vertex importance based on spatial density.

A limitation of the model is that the model predictions are based on a population of young men and women from the United States. The current model is based on an anthropometrically diverse population and appears to perform well for a wide range of head types, but more work is needed to assess the quality of the predictions for markedly different populations. Some national populations are known to have head shapes that differ on average from the rest of the world (e.g., Ball et al. 2010). More data is needed to create a model that works well for a population with different origins than our source data, such as East Asian. Additional data are needed to create useful models of children as well as elderly and obese adults. As a future work, we will analyze the ethnicity and age effects and establish the prediction capability via the online model, once the analysis has been performed with more data.

CONCLUSION

We presented a new parametric head shape model that accounts for head shape variance by analyzing scalp surface data. High-resolution head scans from a diverse sample of female and male adults were used to build the model. The large sample of 3D scans with scalp surface and a broad set of standardized landmarks is a unique attribute of this model. This parametric model opens opportunities to generate a sample of realistic head shapes with a set of landmarks that match a given target anthropometric range to test the product's accommodation.

The parametric head model described here is one of several outcomes of a larger project to solve problems identified by Zehner et al. (2011). The authors pointed out that: (1) measurements from head scans are different from caliper measurements, (2) hair under the cap [donned for scanning] makes the head shape questionable, and (3) female head scans are nearly unusable due to hair volume.

A count by one of us (BDC) estimates there are about 50,000 head scans worldwide that have been taken since the early 1990s when head scanners became widely available. Nearly all of those legacy scans were collected with contactless laser, structured light, or stereo-photo systems. Which means, all those scans suffer from not really knowing scalp shape under the subject's hair.

A follow-on goal for this work is to establish a correspondence between scalp surface and known surfaces in a head scan, essentially from the ears forward and from hairline to chin. With that correspondence, we can then estimate scalp shape for legacy head scans. Zehner et al. (2011) described the shortcomings of head scans for informing helmet design. By predicting the scalp surface, scans will have a minimum head surface (face with scalp), a middle surface- face with compressed hair under a cap, and a maximum surface head scan with no cap (if the scanner was able to capture hair). Alternatively, the three layers may be a face with scalp, head with compressed hair under a cap, and a head with a donned helmet. However, the various head surfaces are combined; an accurate estimation of the scalp's surface makes head scans far more useful in headgear design and performance analysis.

Currently, the three-variable parametric head shape model is publicly available online at http://humanshape.org/head/. The online model provides the essential functionality of the model, such as the rapid generation of a specific head shape model along with the landmark and anthropometric dimension estimation. Users can download the resulting head geometry and estimated dimension data in widely used formats. We anticipate adding more head scans and measurement data in the near future to make the model represent a wider population range.

ACKOLEDGEMENT

This paper was approved for public release USMC MCSC-PRR-3221 and the USAF Public Affairs Clearance 2020-0040.

REFERENCES

Ball, R., Shu, C., Xi, P., Rioux, M., Luximon, Y., & Molenbroek, J. (2010). A comparison between Chinese and Caucasian head shapes. *Applied ergonomics*, *41*(6), 832-839.

Corner, B. D., Beecher, R. M., & Paquette, S. (1997, March). Computer-aided fit testing: an approach for examining the user/equipment interface. In Three-Dimensional Image Capture (Vol. 3023, pp. 37-47). International Society for Optics and Photonics.

Danckaers, F., Lacko, D., Verwulgen, S., De Bruyne, G., Huysmans, T., & Sijbers, J. (2017, July). A combined statistical shape model of the scalp and skull of the human head. In *International Conference on Applied Human Factors and Ergonomics* (pp. 538-548). Springer, Cham.

Friess, M., & Bradtmiller, B. (2003). *3D head models for protective helmet development* (No. 2003-01-2176). SAE Technical Paper.

Gordon CC, Blackwell CL, Bradtmiller B, Parham JL, Hotzman J, Paquette SP, Corner BD, Hodge BM (2013) 2010 Anthropometric Survey of Marine Corps Personnel: Methods and Summary Statistics. NATICK/TR-13/018. Natick, MA: U.S. Army Natick Research, Development, and Engineering Center.

Gordon, C. C., Blackwell, C. L., Bradtmiller, B., Parham, J. L., Barrientos, P., Paquette, S. P., ... & Mucher, M. (2014). *2012 Anthropometric Survey of Marine Corps Personnel: Methods and Summary Statistics.* (No. NATICK/TR-15/007). ARMY NATICK SOLDIER RESEARCH DEVELOPMENT AND ENGINEERING CENTER MA.

Gotoa, L., Leea, W., Songa, Y., Molenbroeka, J., & Goossensa, R. (2015, August). Analysis of a 3D anthropometric data set of children for design applications. In *Proceedings 19th Triennial Congress of the IEA* (Vol. 9, p. 14).

Jolliffe, I. K. (2002) Principal Components Analysis, Second Edition. Springer:New York.

Kouchi, M., & Mochimaru, M. (2004). Analysis of 3D face forms for proper sizing and CAD of spectacle frames. *Ergonomics*, *47*(14), 1499-1516.

Lacko, D., Huysmans, T., Parizel, P. M., De Bruyne, G., Verwulgen, S., Van Hulle, M. M., & Sijbers, J. (2015). Evaluation of an anthropometric shape model of the human scalp. *Applied ergonomics*, *48*, 70-85.

Lacko, D., Vleugels, J., Fransen, E., Huysmans, T., De Bruyne, G., Van Hulle, M. M., ... & Verwulgen, S. (2017). Ergonomic design of an EEG headset using 3D anthropometry. *Applied ergonomics*, *58*, 128-136.

Li, Z., Park, B. K., Liu, W., Zhang, J., Reed, M. P., Rupp, J. D., ... & Hu, J. (2015). A statistical skull geometry model for children 0-3 years old. *PloS one*, *10*(5), e0127322.

Liu, H., Li, Z., & Zheng, L. (2008). Rapid preliminary helmet shell design based on three-dimensional anthropometric head data. *Journal of Engineering Design*, *19*(1), 45-54.

Marin, R., Melzi, S., Rodolà, E., & Castellani, U. (2018). Farm: Functional automatic registration method for 3d human bodies. In *Computer Graphics Forum*.

Mullenger, C.R. & Hudson, J.A. (2015). Female Calvaria Shape Digitization: A Method to Create a Database of Scalp Shapes to be Used in Equipment Design. *DTIC Special Report*.

Park, B. K. D., Ebert, S., & Reed, M. P. (2017). A parametric model of child body shape in seated postures. *Traffic injury prevention*, *18*(5), 533-536.

Park, B. K., Lumeng, J. C., Lumeng, C. N., Ebert, S. M., & Reed, M. P. (2015). Child body shape measurement using depth cameras and a statistical body shape model. *Ergonomics*, *58*(2), 301-309.

Park, B. K., & Reed, M. P. (2015). Parametric body shape model of standing children aged 3–11 years. *Ergonomics*, *58*(10), 1714-1725.

Park, B. K. D., Ebert, S., & Reed, M. P. (2017). A parametric model of child body shape in seated postures. *Traffic Injury Prevention*, 1-4.

Reed, M.P. and Park, B.K.D (2017). Comparison of boundary manikin generation methods. *Proc. 5th International Digital Human Modeling Symposium.* Bonn, Germany.

Shah, P., & Luximon, Y. (2018). Three-dimensional human head modelling: a systematic review. *Theoretical issues in ergonomics science*, *19*(6), 658-672.

Turk, M., & Pentland, A. (1991). Eigenfaces for recognition. *Journal of cognitive neuroscience*, *3*(1), 71-86.

Willinger, R., Diaw, B. M., Baumgartner, D., & Chinn, B. (2002). Full face protective helmet modelling and coupling with a human head model. *International journal of crashworthiness*, *7*(2), 167-178.

Xi, P., & Shu, C. (2009). Consistent parameterization and statistical analysis of human head scans. *The visual computer*, *25*(9), 863-871.

Yang, B., Tse, K. M., Chen, N., Tan, L. B., Zheng, Q. Q., Yang, H. M., ... & Lee, H. P. (2014). Development of a finite element head model for the study of impact head injury. *BioMed research international*, *2014*.

Zehner, G., Metzger, T., & Selby, M. (2011). Creation of a 3-D scan database for helmet design. *SAFE Conference,* 2011, Reno, NV.

Zhuang, Z., Shu, C., Xi, P., Bergman, M., & Joseph, M. (2013). Head-and-face shape variations of US civilian workers. *Applied ergonomics*, *44*(5), 775-784.

APPENDIX A. Landmark Definitions

Name	Definition	Name	Definition
Endocanthion	A bilateral point located at the medial corner of the eye where the upper and lower eyelids meet.	**Subnasale**	The point where the nasal septum merges with the upper cutaneous lip in the mid-sagittal plane.
Exocanthion	A bilateral point located at the lateral corner of the eye where the upper and lower eyelids meet.	**Alar Curvature**	The alar curvature point is a bilateral landmark located at the most posterolateral position along the crease
Infraorbitale	Lowest point on the inferior margin of the boney orbit	**Subalare**	Subalare is a bilateral landmark located below the nostril opening at the point where the infero-medial continuation of the alar cartilage inserts into the skin of the upper lip.
Eye Center,	Estimate center of eye Margin of boney orbit at lateral position of center of eye	**Nasal width**	Points defines the border of nose on the crossline through left and right infraorbitale.

Eyebrow Ridge	Four points evenly distributed along the left /right eyebrow ridge (supraorbital foramen), starting from the most medial point.	**Labiale Superius.** **Stomion** **Labiale Inferius** **Sublabiale**	***Labiale superius*** is located in the midline along the vermillion border of the upper lip. ***Stomion*** is located along the labial fissure in the midline when the lips are closed. ***Labiale inferius*** is located in the midline along the inferior vermillion border of the lower lip. ***Sublabiale*** the most posterior midpoint on the labiomental soft tissue contour that defines the border between the lower lip and the chin.
Pogonion (Anterior Chin point)	The most anterior point on the contour of chin in the midsagittal plane	**Chelion**	**Chelion** is a bilateral landmark located at the outermost corner (commissure) of the mouth where the upper and lower lips meet.
Glabella	A point located at the middle of eyebrows	**Tragion**	***Tragion*** is the point located at the upper margin of each tragus.
Sellion **Rhinion** **Supratip** **Pronasale**	***Sellion*** is located at the deepest depression of the nasal bones at the top of the nose. ***Pronasale*** is defined as the most forward point on the nose tip in the midline. ***Rhinion*** and ***Supratip*** are located at second quarter and third quarter locations between the Sellion and Pronasale.	**Preaurale** **Superaurale** **Subaurale** **Postaurale**	***Preaurale*** is the most anterior point of the ear, located at the level of the helix attachment to the head. ***Superaurale*** is the highest point on the free margin of the auricle ***Subaurale*** is the lowest point on the free margin of the ear lobe. ***Postaurale*** is the most posterior point on the free margin of the ear.
Gnathion	Gnathion is a midline point located on the inferior surface of the chin (mandible).		

APPENDIX B. Head Dimension Definitions

- **Head length**: The distance from the glabella landmark between the brow ridges to the rearmost point of the skull.
- **Face width**: the distance between exocanthions--the outer corners--of the eye.
- **Tragion to Top of the Head (TTOH):** The vertical distance between the right tragion landmark and the horizontal plane tangent to the top of the head. As measured with an anthropometer.
- **Bitragion width**: the distance between the left and right tragion.
- **Ear height**: the distance between the sub-aurale to the super-aurale on each ear.
- **Head circumference**: the length of the intersection of the head surface and the plane perpendicular to the midsagittal plane and going through the glabella and ophistokranion.
- **Arc length**: the arc over the surface of the head, measured from the glabella to the occiput.
- **Arc width**: the arc over the surface of the head, measured from the right tragus to the left tragus.
- **Bitragion chin arc**: the surface distance between the left and right tragion across the anterior point of the chin.
- **Bitragion submandibular arc**: the surface distance between the right and left tragion across the submandibular landmark at the juncture of the jaw and the neck.